fluoroacetic acid (0.124 g, 1.088 mmol) at −40 °C. The temperature of the stirring mixture was allowed to rise to room temperature, and stirring was continued for 1 h. Hexane (50 mL) being added, the mixture was concentrated to dryness. The residue was washed with hexane to remove the unreacted acid, leaving a pale brown powder from which a white powder was sublimed at 110–140 °C (5mmHg). This was identified as dimethyl dihydroxymaleate by compairing the IR and ^{1}H NMR spectra and melting point with those of the authentic sample;[33] mp 150 °C (sublimed) lit. above 150 °C (sublimed). The yield was 0.065 (68%).

The hydrolysis of **10b** in methylene chloride with dry HCl or reduction with $NaBH_4$ in ethanol gave no identifiable product.

Reaction of $PtO_2[P(c\text{-}C_6H_{11})_3]_2$ with $CH_3C{\equiv}CCN$. To a solution of $PtO_2[P(c\text{-}C_6H_{11})_3]_2$ (0.376 g, 0.477 mmol) in methylene chloride was added 1-cyanopropyne[34] (0.034 g, 0.518 mmol) at −40 °C under stirring. The temperature was allowed to reach 0 °C and stirring was continued at 0 °C for 1.5 h. The initial pale yellow turned to light orange. After being stirred for 5 h at ambient temperature, the solution was poured into hexane (80 mL) to yield a yellow powder **11** which was filtered off, washed with hexane (10 mL) three times and dried in vacuo. The yield was 0.299 g (0.351 mmol, 73%), mp 166–168 °C dec. **11** was characterized by elemental analysis, IR, and ^{1}H and ^{13}C NMR spectroscopies. The results are consistent with a formula as $\overline{PtO(CH_3)C{=}CO(CN)}$-$[P(c\text{-}C_6H_{11})_3]$ similar to **10** (see text).

Similar reaction of $PtO_2(PPh_3)_2$ with 1-cyanopropyne in methylene chloride gave an yellow powder whose IR spectrum and elemental analysis confirmed a cyclic adduct analogous to **11**.

Attempts to hydrolyze **11** with trifluoroacetic acid gave the platinum(II) complex $Pt(OCOCF_3)_2[P(c\text{-}C_6H_{11})_3]_2$ and a mixture of red oily untractable substances.

Activation Barriers for Heterogeneous and Homogeneous Electron Transfer. Experimental Tests for Marcus Theory in the Oxidation of Organometallic Complexes

R. J. Klingler and J. K. Kochi*

Contribution from the Department of Chemistry, Indiana University, Bloomington, Indiana 47405. *Received January 26, 1981*

Abstract: Electron transfer is carried out both chemically and electrochemically from four structurally diverse classes of organometallic complexes including those with octahedral, square-planar, tetrahedral, and linear structures. The activation free energies $\Delta G_h^{\ddagger}$ and $\Delta G_e^{\ddagger}$ for the homogeneous and heterogeneous rate processes, respectively, are linearly correlated, provided they are evaluated at the same thermodynamic driving force (i.e., potential). Indeed, the slope of the correlation (Figure 7) is precisely unity when the quadratic Marcus equation describes the free-energy relationship required to span the potential gap between the homogeneous and the heterogeneous rate data. The concordance of the homogeneous and heterogeneous rate processes for organometals is also shown (Figure 9) by the direct correlation of the potential dependences of $\Delta G_h^{\ddagger}$ and $\Delta G_e^{\ddagger}$, as given by the Brønsted coefficient α and the transfer coefficient β, respectively. The observation of second-order effects, as slight curvatures in the potential dependences of α and β (i.e., $\partial\alpha/\partial\Delta G_h$ and $\partial\beta/\partial\Delta G_e$), provides a further, critical test of the Marcus theory.

Introduction

Activation barriers for electron transfer are well provided for by the Marcus theory, particularly as it applies to outer-sphere processes.[1] Heretofore most of the studies of electron transfer have been carried out homogeneously with the chemical oxidants and reductants both in solution. Although there exist some electrochemical comparisons of heterogeneous electron-transfer processes, there are only a limited number of examples in which electron-transfer theories have enabled the clean correlation of the electrochemistry with the chemical rates.[2]

To achieve a direct comparison of the activation barriers for homogeneous and heterogeneous processes, at least two important experimental conditions must be met. First, the chemical oxidants (or reductants) must possess well-defined structural and electron-acceptor (donor) characteristics, and they must be kinetically and electrochemically well behaved. Second, methods must be readily available for the measurements of their heterogeneous electron-transfer rates at various applied potentials. Indeed, we recently showed that the chemical and the anodic oxidations of a homologous series of alkylmetals of tin, lead, and mercury fulfil these requirements.[3] Coupled with the studies of alkylplatinum complexes and organocobalt macrocycles,[4] we now have at our disposal a prescribed series of four structurally diverse classes of organometals, in which the configuration and the coordination about the metal vary systematically from octahedral, square planar, tetrahedral, to linear, as illustrated (I–IV). Each of these organometallic complexes is substitution stable, sufficient to allow meaningful kinetic and electrochemical measurements to be made.

Results

In the following oxidations, we have compared the electrochemical and chemical rate measurements at 25 °C in degassed acetonitrile as the common solvent, and in the presence of tetraethylammonium perchlorate (TEAP) to maintain constant ionic strength or to serve as the supporting electrolyte.

I. Kinetics of the Heterogeneous Oxidation of Organometals at the Platinum Electrode. Anodic oxidation of the organometals

(1) (a) Marcus, R. A. *J. Chem. Phys.* **1956**, *24*, 966. (b) For reviews see: Reynolds, W. L.; Lumry, R. W. "Mechanisms of Electron Transfer"; Ronald Press: New York, 1966. Sutin, N. In "Inorganic Biochemistry"; Eichhorn, G. L., Ed.; Elsevier: Amsterdam, 1973; Vol. 2, p 611. Pennington, D. E. *ACS Monogr.* **1978**, No. 174, 477. Cannon, R. D. "Electron Transfer Reactions"; Butterworths: New York, 1980.

(2) See, for example: (a) Peover, M. E. In "Reactions of Molecules at Electrodes"; Hush, N. S., Ed.; Wiley-Interscience: London, 1971; p 259. (b) Hale, J. M., *Ibid.*, p 229. (c) Saji, T.; Maruyama, Y.; Aoyagui, S. *J. Electroanal. Chem.* **1978**, *86*, 219. (d) Weaver, M. J. *J. Phys. Chem.* **1980**, *84*, 568. (e) Kojima, H.; Bard, A. J. *J. Am. Chem. Soc.* **1975**, *97*, 6317.

(3) Klinger, R. J.; Kochi, J. K. *J. Am. Chem. Soc.* **1980**, *102*, 4790. Note that the heterogeneous rate constant k_e is expressed in units of cm s^{-1}.

(4) (a) Chen, J. Y.; Kochi, J. K. *J. Am. Chem. Soc.* **1977**, *99*, 1450. (b) Chen, J. Y.; Gardner, H. C.; Kochi, J. K. *Ibid.* **1976**, *98*, 6150. (c) Tamblyn, W. H.; Klingler, R. J.; Hwang, W. S.; Kochi, J. K. *Ibid.* **1981**, *103*, 3161.

(5) Wong, C. L.; Kochi, J. K. *J. Am. Chem. Soc.* **1979**, *101*, 5593.

(6) Fukuzumi, S.; Wong, C. L.; Kochi, J. K. *J. Am. Chem. Soc.* **1980**, *102*, 2928.

0002-7863/81/1503-5839$01.25/0 © 1981 American Chemical Society

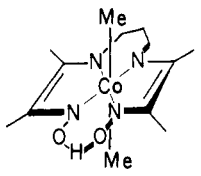

I

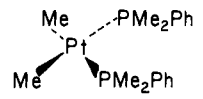

II

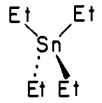

III

Et-Hg-Me

IV

I–IV affords organometal cations which have lifetimes less than 1 ms, rendering the electrochemical process irreversible.[3,4c] The heterogeneous rates of electron transfer in eq 1 were measured

$$RM \xrightarrow{k_e} RM^+ + e^- \qquad (1)$$

by two independent electrochemical methods: cyclic voltammetry and convolutive linear sweep voltammetry. The utility of the first method stems from its simplicity, while that of the second derives from its rigor, as discussed in the sections immediately following.

A. Cyclic Voltammetry (CV) of Organometals. The single-sweep cyclic voltammograms of the organometals listed in Table I were recorded with a stationary platinum microelectrode in acetonitrile solutions at 25 °C with TEAP as the supporting electrolyte. The cyclic voltammogram of the dimethylplatinium-(II) complex $Me_2Pt(PMe_2Ph)_2$ is illustrated in Figure 1 at various scan rates. It is characterized by an anodic wave showing a well-defined current maximum, but no cathodic wave on the reverse scan even at sweep rates up to 10 V s^{-1} and temperatures as low as −80 °C. The cyclic voltammograms of the other organometals in Table I are also characterized by the same basic patterns. Indeed, independent analysis has shown that the rate of the decomposition of the oxidized organometal cation is sufficiently rapid to render the forward electron-transfer step in eq 1 as the rate-limiting process in an otherwise fast kinetic scheme.[4] Under these conditions, the heterogeneous rate constant for electron transfer at the CV peak potential E_p has been shown to be given by[3]

$$k_e(E_p) = 2.18\left[\frac{D\beta nFv}{RT}\right]^{1/2} \qquad (2)$$

where n is the number of electrons transferred in the rate-limiting step, and v is the scan rate. The diffusion coefficient D and the transfer coefficient β are measured by independent techniques, as described previously.[3] Equation 2 is derived from Fick's laws of diffusion together with the usual expression for the potential dependence of the heterogeneous rate constant k_e for electron transfer,[7]

$$k_e(E) = k_s \exp\left[\frac{\beta nF}{RT}(E - E^0)\right] \qquad (3)$$

where E^0 is the standard potential for the organometal which fixes the value of k_s.[8]

The shift in the current maximum with the sweep rate in Figure 1 accords with standard electrochemical theory[9,10] and may be used with the aid of eq 2 to determine the heterogeneous rate constants k_e for electron transfer at different values of the applied potential. The results of this analysis are shown in Figure 2 for the representative classes of organometals I–IV.[11] The plots in Figure 2 correspond to the linear free-energy relationship in eq 3, with the slope representing the electrochemical transfer coefficient β, i.e.,

$$\beta = \frac{2.3RT}{nF}\left(\frac{\partial \log k_e}{\partial E}\right) \qquad (4)$$

A closer scrutiny of Figure 2 reveals the persistence of small, but consistent curvatures in all of the plots. In order to verify the curvature, the transfer coefficient β was also determined inde-

Table I. Cyclic Voltammetric Data for Alkylmetals[a]

alkylmetal	E_p[b] (V)	β[c]	D (10^5 cm^2 s^{-1})	$-\log k_e$[e] (cm s^{-1})	$\Delta G_e^{\ddagger}$[h] (kcal mol^{-1})
$Me_2Co(DpnH)$[f]	0.43	0.73	1.5	1.85	7.44
$Me_2Co(TIM)^+$[g]	0.32	0.58	1.3	1.93	7.55
$MeCo(DpnH)^+$	1.57	0.58	1.4	1.91	7.53
$EtCo(DpnH)^+$	1.43	0.74	1.4	1.86	7.46
$Me_2Pt(PMe_2Ph)_2$	1.08	0.26	*d*	2.04	7.71
$Me_2Pt(PMe_2C_6H_4CF_3)_2$	1.22	0.27	*d*	2.03	7.69
Me_4Sn	2.55	0.29	*d*	2.02	7.68
Et_4Sn	1.82	0.33	1.8	1.98	7.62
$i\text{-}Pr_4Sn$	1.58	0.29	1.8	2.01	7.66
$n\text{-}Bu_4Sn$	1.82	0.32	1.7	2.00	7.65
$i\text{-}Bu_4Sn$	1.85	0.26	1.9	2.02	7.68
$(neopentyl)_4Sn$	1.87	0.31	*d*	2.00	7.65
Et_4Pb	1.33	0.31	*d*	2.00	7.65
EtHgMe	1.78	0.20	*d*	2.03	7.69

[a] Measured with a stationary platinum microelectrode at 100 mV s^{-1} in acetonitrile containing tetraethylammonium perchlorate as supporting electrolyte at 25 °C. [b] Potential relative to saturated NaCl-SCE. [c] Calculated from the width of the wave according to eq 5. [d] A value of 1.7×10^{-5} cm^2 s^{-1} was used. [e] Calculated according to eq 2. [f] DpnH = 2,3,9,10-tetramethyl-1,4,8,11-tetraazaundeca-1,3,8,10-tetraen-11-ol-1-olate. [g] TIM = 2,3,9,10-tetramethyl-1,4,8,11-tetraazacyclotetradeca-1,3,8,10-tetraene. [h] Calculated from eq 14 with $Z_e = 3.5 \times 10^3$ cm s^{-1}.

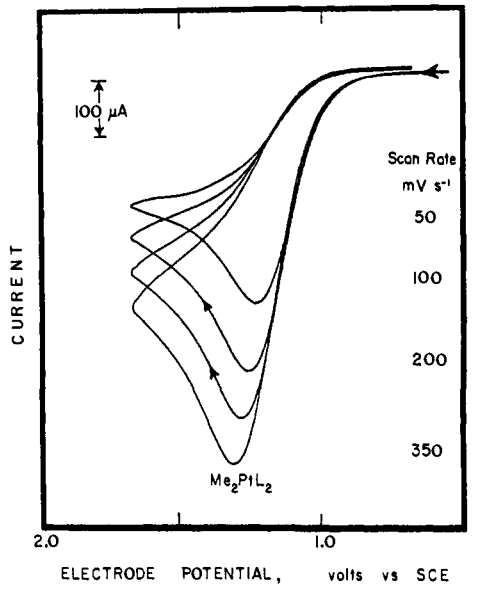

Figure 1. Single-sweep cyclic voltammograms at various scan rates of 8×10^{-3} M $Me_2Pt(PMe_2Ph)_2$ in acetonitrile solutions containing 0.1 M TEAP at 25 °C.

(7) Bauer, H. H. *J. Electroanal. Chem.* **1968**, *16*, 419.

(8) (a) Equation 2 was developed for the limiting case of total electrochemical irreversibility, i.e., rate-limiting electron transfer.[3] For the evaluation of the small errors possibly arising from partial reversibility, see Klingler, R. J.; Kochi, J. K. *J. Phys. Chem.* **1981**, *85*, 1731. (b) Second-order terms of the magnitude observed with organometals (vide infra) will introduce only negligible error in the application of eq 2.

(9) Nicholson, R. S.; Shain, I. *Anal. Chem.* **1964**, *36*, 706.

(10) (a) Delahay, P. *J. Am. Chem. Soc.* **1953**, *75*, 1190. (b) Matsuda, H.; Ayabe, Y. *Z. Elektrochem.* **1955**, *59*, 494. (c) Nadjo, L.; Saveant, J. M. *Electroanal. Chem.* **1973**, *48*, 113.

(11) The values of log k_e were calculated from the data in ref 3 and 4c.

Table II. Heterogeneous Rate Constants for Electron Transfer from the Cyclic Voltammetric (CV) and the Convolutive Potential Sweep Voltammetric (CPSV) Methods[a]

organometal	E,[b] V vs. SCE	$\log k_e$ CV[c]	$\log k_e$ CPSV[d]	β CV[e]	β CPSV[f]	$-\partial\beta/\partial E$ CV[e]	$-\partial\beta/\partial E$ CPSV[f]
Et_4Sn	1.65	−2.26	−2.14	0.37 ± 0.05	0.31 ± 0.05	0.8 ± 0.2	1.4 ± 0.2
i-Bu_4Sn	1.82	−2.23	−2.01	0.30 ± 0.05	0.28 ± 0.05	0.8 ± 0.2	0.7 ± 0.2
sec-Bu_4Sn	1.50	−2.60	−2.53	0.29 ± 0.05	0.28 ± 0.05	0.7 ± 0.2	1.0 ± 0.2

[a] Measured at a stationary platinum microelectrode at 25 °C in acetonitrile containing 0.1 M TEAP. [b] Chosen at the centers in Figure 3. [c] From eq 2. [d] From eq 6. [e] From the width of the CV wave according to eq 5. [f] From figure 4 using eq 4.[16]

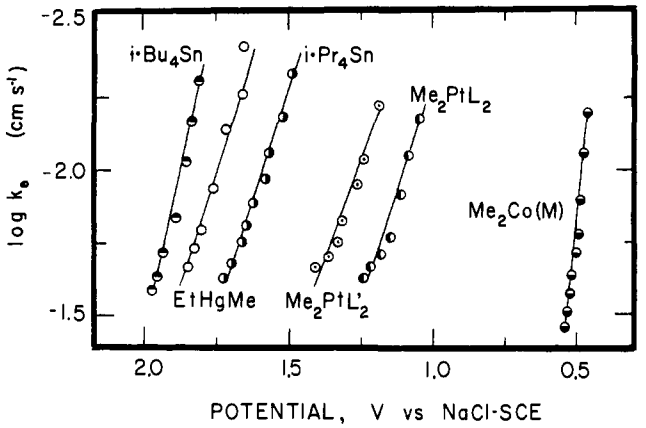

Figure 2. Variation of the heterogeneous rate constant k_e for electron transfer with the applied electrode potential E for representative organometals in acetonitrile solutions containing 0.1 M TEAP at 25 °C. The ligand designations are: L = PMe_2Ph, L' = $PMe_2C_6H_4CF_3$-p, (M) = DpnH.

pendently from the width of the CV wave, as described by Nicholson and Shain,[9] i.e.,[12]

$$\beta = \frac{1.857RT}{nF}[E_p - E_{p/2}]^{-1} \qquad (5)$$

The potential dependence of β obtained in this manner is shown in Figure 3.[13] The slopes $\partial\beta/\partial E$ represent the unmistakable presence of curvature in Figure 2. [The curves in Figure 2 were also fitted by a least-squares treatment to a second-order polynomial, the second-order terms of which are identical with the slopes in Figure 3.]

The cyclic voltammetric determination of the heterogeneous rate constants for electron transfer from eq 2 relies on the assumption that the free-energy relationship in eq 3 is effectively linear over the width of the CV wave. However, the results in Figures 2 and 3 indicate the free-energy relationship is not truly linear over an extended potential range. Therefore, we deemed it necessary to confirm the CV results by the alternate method using convolutive potential sweep voltammetry, which requires no assumptions as to the form of the free-energy relationship and is ideally suited for an independent analysis of the curvature revealed in Figure 3.

B. Convolutive Potential Sweep Voltammetry (CPSV) of Organometals. In convolutive linear sweep voltammetry,[14] the heterogeneous rate constant for rate-limiting electron transfer k_e is obtained from the current $i(E)$ at a given applied potential by using the equation

$$k_e(E) = (nFA)^{-1}\frac{i(E)}{C(t)} \qquad (6)$$

where A is the area of the electrode, and $C(t)$ is the time-dependent concentration of the electroactive (organometal) species at the electrode surface. The values of $C(t)$ can be evaluated, as described in the Experimental Section, from the current–time history using the convolution integral

$$C(t) = C^0\left[1 - \pi^{-1/2}\int_0^t \frac{i(\eta)}{(t-\eta)^{1/2}}\,d\eta\right] \qquad (7)$$

where C^0 is the initial concentration of the organometal in the bulk solution. It is important to emphasize that eq 7 is kinetically rigorous, since it derives directly from Fick's laws of diffusion and assumes no explicit form for the heterogeneous rate constant for electron transfer k_e. Rather, k_e is obtained directly from an experimental measurement of the current arising from a linear sweep of the potential.[15]

The heterogeneous rate constants obtained by the CPSV method are plotted in Figure 4a at various electrode potentials. The curvature in the free-energy relationship is best seen by plotting the instantaneous slopes ($\partial \log k_e/\partial E$), as in Figure 4b.[16]

The results in Table II show that the CPSV method affords values of the heterogeneous rate constants, transfer coefficients, and curvatures which are all in excellent agreement with those obtained from the CV method.[17] We are thus assured that the kinetic parameters in Table I, obtained from the convenient CV method, represent reliable values of the heterogeneous rate constants and transfer coefficients.

II. Kinetics of the Homogeneous Oxidation of Organometals with Iron(III) and Iridium(IV) Oxidants. The kinetics of the homogeneous chemical oxidation of the various organometals RM were examined earlier with a series of iron(III) complexes,

$$RM + FeL_3^{3+} \xrightarrow{k_h} RM^+ + FeL_3^{2+} \qquad (8)$$

where L = substituted 1,10-phenanthrolines.[5] All the oxidation reactions obeyed second-order kinetics, being first order in each reactant, i.e.,

$$-\frac{d[RM]}{dt} = k_h[RM][FeL_3^{3+}] \qquad (9)$$

where RM represents the dimethylcobalt(III) macrocycles, dimethylbis(phosphine)platinum(II), or the series of tetraalkyltin(IV) and dialkylmercury(II) complexes, I–IV. In each case, the second-order rate constants k_h relisted for convenience in Table I-S (in the Supplementary Material) were consistent to within 10%. For comparison, some of the rate constants for the oxidation of the same organometals by hexachloroiridate(IV), are also included from related studies.[4]

$$RM + IrCl_6^{2-} \xrightarrow{k_h} RM^+ + IrCl_6^{3-} \qquad (10)$$

(12) Curvature in the free-energy relationship may also be measured by a detailed comparison of the shape of the CV wave by digital simulation [Corrigan, D. A.; Evans, D. H. *J. Electroanal. Chem.* **1980**, *106*, 287].

(13) (a) The transfer coefficients β were calculated from the width of the wave according to eq 5 using the data in ref 3 and 4c. (b) The transfer coefficient is plotted in Figure 3 at the average potential of the CV wave, given by $E = {}^1/_2(E_p + E_{p/2})$.

(14) Imbeaux, J. C.; Saveant, J. M. *J. Electroanal. Chem.* **1973**, *44*, 169. Saveant, J. M.; Tessier, D. *J. Phys. Chem.* **1978**, *82*, 1723.

(15) At the low sweep rates employed in these studies, complications arising from the charging current are minimal.

(16) In order to reduce the scatter incurred by calculating instantaneous slopes, values of $\Delta\Delta\log k_e/\Delta E$ from five contiguous data points in Figure 4a were averaged for each point shown in Figure 4b.

(17) This conclusion is not completely unexpected, since the CV method summarized by eq 2 can be derived from eq 6. Thus, Nicholson and Shain[9] have shown for linear sweep voltammetry that the current peak i_p will occur when the concentration $C(t)$ has dropped to 22.7% of C^0. Proceeding from eq 6, it then follows that $k_e(E_p) = (nFA)^{-1}i_p/0.227C^0$, which is identical with eq 2, since the peak current is given by[9] $i_p = 0.4958\ nFAC^0(DnFv/RT)^{1/2}$.

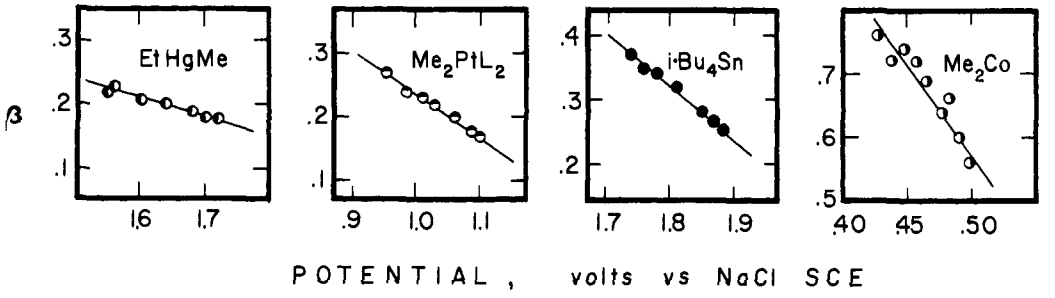

Figure 3. Dependence of the heterogeneous transfer coefficient β with the applied electrode potential E for the representative class of organometals I–IV.

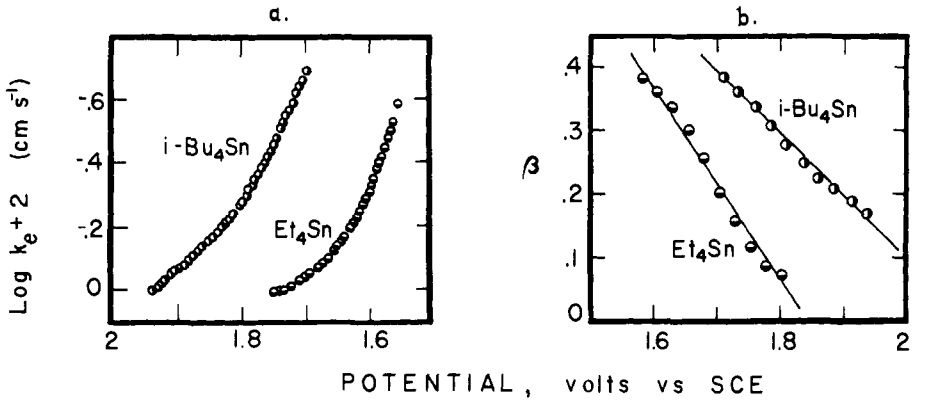

Figure 4. Left: Heterogeneous rate constants k_e measured by convolutive potential sweep voltammetry at various electrode potentials in acetonitrile. Right: Transfer coefficients obtained from the intantaneous slopes in (a), as described in the text.

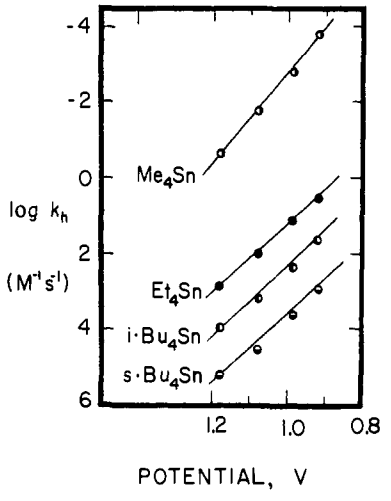

Figure 5. Variation of the homogeneous rate constant (log k_h) for electron transfer with the standard reduction potential E^0 of the iron(III) oxidant using representative organometals in Table II-S.

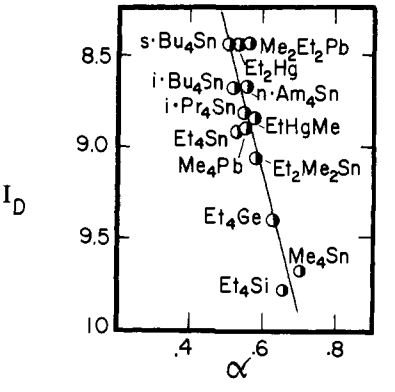

Figure 6. Dependence on the homogeneous Brønsted slope α on the ionization potential I_D of the organometal from ref 6. The values of α were calculated by the least-squares fit of the data in Table II-S.

The linear variation of the electron-transfer rate constant log k_h with potential E^0 of the iron(III) oxidant is shown in Figure 5. The correlations represent a linear free-energy relationship of the form: log $k_h \propto E^0$, in which the slope corresponds to the Brønsted coefficient α, i.e.,

$$\alpha = \frac{2.3RT}{nF}\left(\frac{\partial \log k_h}{\partial E^0}\right) \qquad (11)$$

A close scrutiny of the plots in Figure 5 (from top to bottom) reveals that the magnitudes of the slopes α generally decrease with increasing reactivity of the alkyltin compound. Indeed, Figure 6 shows that α increases monotonically with the electron-donor property of the organometal, as measured by its ionization potential I_D. [For this series of alkyltin compounds, the ionization potential in the gas phase is related to the oxidation potential in acetonitrile solution by a multiplicative factor of 1.8.[6]] It is noteworthy that the slope in Figure 6 represents $\partial\alpha/\partial E^0$, and as such it is directly related to curvature in each of the plots in Figure 5. Indeed, each of the loci points in Figure 5 describes a minuscule curve, and thus the straight lines are only good approximations.

Discussion

The facile oxidation of organometals by both electrochemical as well as chemical means represents an excellent opportunity to compare quantitatively the activation processes for heterogeneous and homogeneous electron-transfer processes. In the following discussion, we have focussed our attention primarily on the homologous series of tetraalkyltin and lead compounds since they represent a class of organometals in which the steric and electron-donor properties can be varied in a well-defined, systematic way.[18]

I. Comparison of the Homogeneous and Heterogeneous Rate Processes for Electron Transfer. The direct comparison of the

(18) Compare Fukuzumi, S.; Mochida, K.; Kochi, J. K. *J. Am. Chem. Soc.* **1979**, *101*, 5961. Fukuzumi, S.; Kochi, J. K. *J. Phys. Chem.* **1980**, *84*, 608, 617.

electrochemical and chemical oxidation of organometals requires that they be evaluated at the same thermodynamic driving force; i.e., the applied electrode potential must be reasonably similar to the standard reduction potential of the chemical oxidant.[19] This situation is unfortunately often difficult to obtain experimentally. For example, the electrochemical currents for the anodic oxidation of tetraalkyltins at the standard reduction potentials of the iron(III) oxidants (ranging from 0.92 to 1.18 V) are too small to be reliably measured. Conversely at the applied electrode potentials convenient for the CV measurements of tetraalkyltins (ranging from 1.5 to 1.9 V), the homogeneous chemical rates of oxidation would be too fast to measure.[20] Since such an experimental dilemma is expected to be commonly encountered, our task is to develop general procedures for carrying out this evaluation.

Basically, the problem is to find the free-energy relationship which will allow the electron-transfer rate constant, measurable at one potential, to be evaluated at another potential. We consider two free-energy relationship: the well-accepted linear form in eq 3[7] and the quadratic Marcus equation.[21]

A. Application of the Linear Free-Energy Relationship. The heterogeneous rate constant (log k_e) is an approximately linear function of the applied potential E, as shown by the plots in Figure 2. The free-energy relationship for an oxidation is quantitatively described by

$$k_e(E) = 2.18\left[\frac{D\beta nFv}{RT}\right]^{1/2} \exp\left[\frac{\beta nF}{RT}(E - E_p)\right] \quad (12)$$

which is obtained from the combination of eq 2 and 3.[3] Indeed this linear free-energy relationship may be used to obtain the heterogeneous rate constants for electron transfer at the standard reduction potentials E^0 of the series of tris(phenanthroline)iron(III) oxidants, which are listed in Table II-S. The heterogeneous rate constants (log k_e) were evaluated with the aid of eq 12 at the E^0 of the iron(III) oxidants, and are tabulated in Table III-S.

The striking linear correlation of the homogeneous rate constant (log k_h) with the heterogeneous rate constant (k_e), when both processes are measured under conditions of equivalent thermodynamic driving force, was presented in the earlier study (see Figure 6 in ref 3). However, the resultant correlation did not have the expected (least-squares) slope of unity, but only a value of 0.74, and an intercept of 4.8 kcal mol^{-1}. For the significance of these parameters, we now turn to the quadratic form of the Marcus theory to provide an alternative free-energy relationship for the heterogeneous rate constants.

B. Application of the Quadratic Marcus Free-Energy Relationship. According to Marcus, the activation free-energy $\Delta G^{\ddagger}$ for outer-sphere electron transfer relates to the standard free-energy change ΔG through an intrinsic barrier $\Delta G_0^{\ddagger}$ in eq 13,[21,24]

$$\Delta G^{\ddagger} = \Delta G_0^{\ddagger}\left(1 + \frac{\Delta G + w^p}{4\Delta G_0^{\ddagger}}\right)^2 \quad (13)$$

where w^p is the work needed to bring the products (or product and electrode) together. For neutral reactants such as the organometals examined in this study, we consider the work term of the reactants to be nil. In order to compare the rates of the heterogeneous electrode processes and the homogeneous chemical oxidations, the rate constants k_e and k_h were converted to the free energies of activation given by:

$$\Delta G^{\ddagger} = -RT \ln (k/Z) \quad (14)$$

where the collision frequency Z for the heterogeneous (Z_e) and the homogeneous (Z_h) rate processes were taken as 3.5×10^3 cm s^{-1} and 3.0×10^{10} M^{-1} s^{-1}, respectively.[22]

In an electrochemical process, the free-energy change for oxidation is:

$$\Delta G = -nF(E - E^0) \quad (15)$$

Values of $(\Delta G + w^p)$ can be calculated from the Marcus eq 13 for various alkylmetals, by using the values of the activation free energy $\Delta G^{\ddagger}$ at the CV peak potential listed in Table I, and the intrinsic barrier $\Delta G_0^{\ddagger}$ evaluated from the transfer coefficient β by[25]

$$\Delta G_0^{\ddagger} = \Delta G^{\ddagger}/4\beta^2 \quad (16)$$

Knowledge of $(\Delta G + w^p)$ at the peak potential, obtained in this way, allows $\Delta G^{\ddagger}$ to be evaluated at any other potential.[27]

The values of $\Delta G_e^{\ddagger}$ evaluated at the standard reduction potentials of the iron(III) oxidants are listed in Table IV-S. The new correlation of the activation free energies shown by the solid line in Figure 7 represents the least-squares fit with a standard deviation of 0.03. More importantly, the slope of 1.01 represents strong support for a common outer-sphere activation mechanism for homogeneous and heterogeneous electron transfer from these organometals. For a detailed elaboration of the significance of the unit slope and the nonzero intercept in Figure 7, see the Experimental Section.

An important feature of the correlation in Figure 7 for the oxidation in eq 8 is the striking absence of steric effects arising from the organometal, particularly with changes in the structures of the alkyl ligand. Thus, increasing the branching of the alkyl

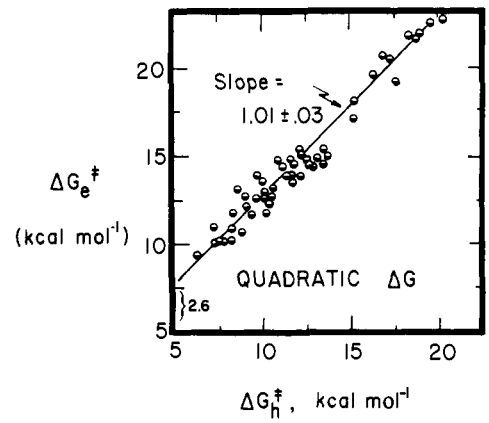

Figure 7. Correlation of the homogeneous activation free energy $\Delta G_h^{\ddagger}$ for iron(III) oxidations and the heterogeneous activation free energy $\Delta G_e^{\ddagger}$ using the quadratic Marcus eq 13.

(19) Such comparisons have typically been carried out by measuring the electrochemical rates of the oxidant and the reductant at their standard reduction potentials, and using a cross relationship such as that given by Marcus.[1] The unavailability of E^0 for organometals precludes such a treatment here.

(20) Provided such oxidants were available.

(21) Marcus, R. A. *J. Phys. Chem.* **1963**, *67*, 853.

(22) The collision frequencies for the heterogeneous and homogeneous electron transfers were calculated using the following expressions: $Z_e = (RT/2\pi M)^{1/2}$ and $Z_h = 10^3 N(8\pi RT/\bar{M})^{1/2} r^2$, where N is Avogadro's number, M the molecular weight, $\bar{M}$ the reduced molecular weight of the reactant pair, and r the distance separating the reactants. An average mass of 350 and a distance of 7×10^8 cm were used to obtain $Z_e = 3.5 \times 10^3$ cm s^{-1} and $Z_h = 3 \times 10^{10}$ M^{-1} s^{-1}.

(23) The homogeneous activation free energy for hexachloroiridate (IV) oxidation of organometals was calculated from the data in ref 5.

(24) (a) Marcus, R. A. *J. Chem. Phys.* **1965**, *43*, 679. (b) The intrinsic barrier is also referred to as the reorganization energy $\lambda = 4\Delta G_0^{\ddagger}$.

(25) (a) The derivation of this equation is included in the Experimental Section. (b) Equation 16 assumes that the heterogeneous work term w^p is effectively a constant with respect to the free-energy change. Thus it has been shown for neutral reactants that the double layer correction at mercury electrodes introduces less than 5% error for potentials over a volt removed from the point of zero charge.[26a] Furthermore, recent differential capacity data in acetonitrile at a platinum electrode give the zero point as −0.15 V vs. NaCl-SCE.[26b] Petri and Khomechenko also found that both the magnitude of the differential capacity and its dependence on the applied potential at platinum was much smaller than at mercury electrodes. Taken together, these observations indicate that the error in assuming w^p to be a constant for the alkylmetals under study will be less than 5%. For a further discussion at this point, see section II, relating to α and β.

(26) (a) Saveant, J. M.; Tessier, D. *J. Phys. Chem.* **1977**, *81*, 2192. (b) Petri, O. H.; Khomechenko, I. G. *J. Electroanal. Chem.* **1980**, *106*, 277.

(27) Note that $\Delta G(E) = \Delta G(E_p) + 23.06(E_p - E)$.

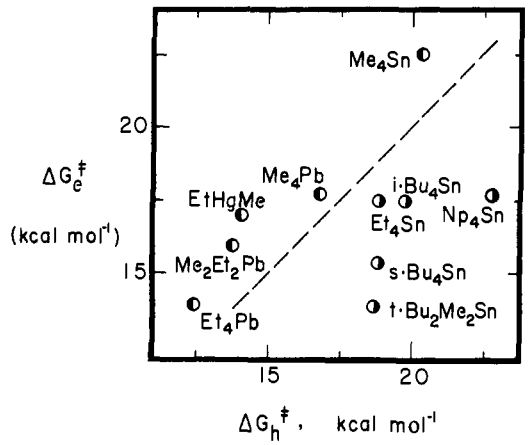

Figure 8. Correlation of the homogeneous activation free energy for hexachloroiridate(IV) oxidation with the heterogeneous activation free energy using the linear free energy relationship in eq 12 from Table III-S. For the significance of the dashed line arbitrarily drawn with a slope of unity and starting at the origin, see text.

ligand at the β carbon with methyl groups in the homologous series CH_3CH_2, $(CH_3)_2CHCH_2$, and $(CH_3)_3CCH_2$ leads to no deviation in the correlation. Even the highly hindered tetraneopentyltin is included precisely with the sterically accessible methylethylmercury. Such an absence of steric influences, coupled with the dominance of the electron donor properties shown in Figures 2 and 5, describes the *outer-sphere mechanism* for electron transfer in which there is minimal interpretation of the coordination spheres in the transition state, schematically depicted in V for the oxidation of tetraethyltin by tris(phenanthroline)iron(III).

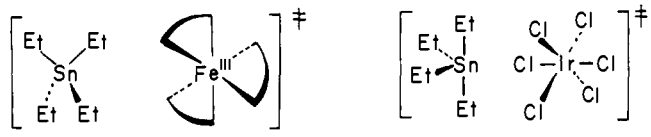

V VI

By way of contrast, a similar comparison of the homogeneous oxidation of the same organometals by hexachloroiridate(IV), in eq 10, with the heterogeneous process fails badly in two important ways. First, the random, "buckshot" appearance of the data in Figure 8 shows no correlation of the activation energies.[23] Second, if the points are compared relative to the dashed line (arbitrarily starting at the origin and drawn with a slope of unity), the organometals fall into two categories: those lying to the left being more reactive chemically than electrochemically, and the opposite being true for those organometals lying to the right of the line. Structurally, the organometals lying to the right of the line are also all more sterically hindered than those lying on the opposite side. Indeed the largest deviations are shown by the sterically congested tetraneopentyltin and di(*tert*-butyl)dimethyltin. Both of these observations indicate the presence of an *inner-sphere interaction* between the organometal and hexachloroiridate(IV), in which steric effects deter the attainment of the transition state, such as in the distorted organometal represented in VI from previous chemical studies.[6] Indeed, the contrast between the divergent patterns in Figures 7 and 8 may be generally applied as a criterion for the outer-sphere mechanism of the primary electron-transfer process.

II. Comparison of Homogeneous Brønsted and Heterogeneous Transfer Coefficients. Historically, the slopes of the free-energy relationships have been referred to separately as the Brønsted coefficient α for homogeneous processes and as the transfer coefficient β for heterogeneous processes.[7,28] The homogeneous Brønsted slopes α in Figure 6 lie in the range from 0.71 to 0.53 for Me_4Sn and *sec*-Bu_4Sn at the extremes of the tetraalkyltin

(28) Kresge, A. J. *Chem. Soc. Rev.* **1973**, *2*, 475.

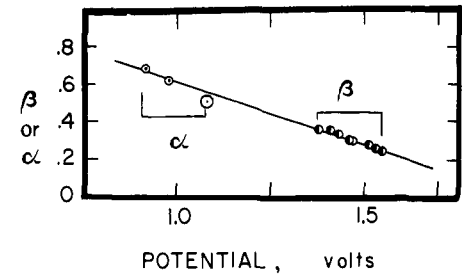

Figure 9. Comparison of the homogeneous Brønsted coefficient α (⊙) and heterogeneous transfer coefficient β (●) for *sec*-Bu_4Sn in acetonitrile.[29] The line represents the least-squares fit of only the heterogeneous β.

reactivities, which we have studied. In contrast, the electrochemical transfer coefficients β of the same organometals in Figure 3 fall in the significantly lower range between 0.20 and 0.35.

Figure 9 includes a plot of α against the standard iron(III) potential, together with that of β against the applied electrode potential.[29] The solid line represents the least-squares fit to only the electrochemical data (β's), using the same slope of $\partial\beta/\partial E = -0.69$ V^{-1} previously evaluated, as in Figure 3. Clearly, the homogeneous iron(III) points (α) fit on this line, as also indicated by the correlation coefficient of 0.99 evaluated from all the data (i.e., β's plus α's). [Note: *sec*-Bu_4Sn is our best example for the demonstration in Figure 9, owing to the minimal potential gap between the electrochemical and chemical data. Although the same correlations are obtained with the other organometals, the small cluster of electrochemical points which are far removed from the chemical data makes the fit of α in the extrapolation less obviously compelling.]

Three important conclusions can be drawn from the analysis in Figure 9. First, the difference between the electrochemical β and the chemical α slopes arises from the fact that the two are measured in different potential regions, necessitated solely by the experimental limitations (vide supra). Otherwise, there is no inherent difference between α and β in the oxidation of these organometals. Second, the importance of the second-order term in the potential, i.e., the curvatures in Figures 2 and 5, is confirmed for both the heterogeneous and the homogeneous rate processes, respectively. Thus a single value of α or β cannot be used to describe both the homogeneous and heterogeneous rate data. Third, the accordance of β with α demonstrates that factors contributing to the potential dependence of the heterogeneous process must be fundamentally the same as than in the homogeneous electron transfer. Thus complications relating specifically to the electrode process, such as the potential dependence of the heterogeneous work term w^p and other double layer effects,[30] are not significant in this system, as indeed assumed in the derivation of eq 16.[25]

III. Evaluation of the Intrinsic Barrier to Electron Transfer. A Comparison of Electron-Transfer Theories. The foregoing discussion has pointed out the importance of the proper free-energy relationship in providing the means to span the potential gap ($E_p - E$) between the homogeneous and heterogeneous rate data—a large potential gap requiring a large extrapolation of the free-energy relationship. Since the intrinsic barrier $\Delta G_0^{\ddagger}$ represents the limit of the extrapolation (i.e., at $\Delta G = 0$), its evaluation represents a severe, critical test for any free-energy relationship to be of predictive value.

(29) After the least-squares fit of the homogeneous rate data in Table II-S to a polynomial of degree two, the first- and second-order coefficients were used to calculate α. See footnote 13a for the determination of β. Note that the error in α at 1.181 V is larger than the others owing to a value of k_h which is at the limit of the stopped-flow measurement.

(30) (a) The heterogeneous work term or Frumkin correction is directly related to the double layer potential φ_r of the reaction plane relative to the bulk solution, as $w^p = z\varphi_r$ where z is the ionic charge. See Delahay, P. ["Double Layer and Electrode Kinetics"; Interscience: New York, 1965; Chapter 2], and ref 26 for a recent evaluaton and discussion. (b) An independent measurement of the effects of the double layer potential in this system is planned.

Table III. Intrinsic Barrier Calculated from Marcus Theory Using the Transfer Coefficient (Eq 16) or the Curvature (Eq 17)

alkylmetal	$\Delta G^{\ddagger}$ (kcal mol^{-1})	β	$\partial\beta/\partial\Delta G$ (kcal^{-1} mol)	$\Delta G_0^{\ddagger}$ (kcal mol^{-1}) eq 16	eq 17	$\Delta\tilde{G}_0^{\ddagger}$[a] (kcal mol^{-1})
Et_4Sn	8.00	0.34	0.032	17	4	8
(*sec*-Bu)$_4$Sn	8.47	0.29	0.032	25	4	10
(*i*-Bu)$_4$Sn	7.97	0.30	0.032	22	4	9

[a] Geometric mean of values in columns 5 and 6.

A. $\Delta G_0^{\ddagger}$ from Marcus Theory. The intrinsic barrier for electron transfer $\Delta G_0^{\ddagger}$ can be obtained in two independent ways from the Marcus eq 13. The first derivative, $\partial\Delta G^{\ddagger}/\partial\Delta G$, yields $\Delta G_0^{\ddagger}$ in terms of the absolute magnitude of the transfer coefficient β (or the Brønsted α), as previously described in eq 16. Alternatively, a second value of $\Delta G_0^{\ddagger}$ may be determined after a subsequent differentiation, in terms of the potential dependence of β (or α) according to eq 17.[31] The values of $\Delta G_0^{\ddagger}$ obtained from the

$$\Delta G_0^{\ddagger} = [8(\partial\beta/\partial\Delta G)]^{-1} \qquad (17)$$

magnitude (eq 16) and from the slope (eq 17) of β or α must be identical for those systems which are adequately described by the quadratic form of the Marcus eq 13. Indeed this may be demonstrated to be the case for the homogeneous iron(III) oxidation in which $\Delta G_0^{\ddagger} = 10 \pm 0.5$ kcal mol^{-1} has been determined from eq 16 for tetraalkyltin.[6] For comparison, the slope of 0.28 V^{-1} in Figure 6 yields a value of 10 ± 0.5 kcal mol^{-1} for $\Delta G_0^{\ddagger}$ when it is inserted into eq 17. The excellent agreement between these two determinations of $\Delta G_0^{\ddagger}$ attests to the ability of the Marcus eq 13 to describe homogeneous electron-transfer rate data for this homologous series of organometals.

As a further test of the Marcus eq 13, we now apply eq 16 and 17 to the electrochemical rate data, which are further removed from the equilibrium potential, as also indicated by the variation of β from 0.5 to ~0.3. The results of the computations from eq 16 and 17 using the experimental data in Table II are presented in Table III, columns 5 and 6, respectively.

The fact that the two determinations of $\Delta G_0^{\ddagger}$ in Table III differ significantly indicates that eq 13 does not provide an adequate functional description for these data. It is noteworthy, however, that the geometric mean $\Delta\tilde{G}_0^{\ddagger}$ included in column 7, is quite comparable to that ($\Delta G_0^{\ddagger} = 10$ kcal mol^{-1}) obtained from the homogeneous rate data.[6] This observation suggests that the magnitude of β is smaller than the value predicted by eq 16, and the slope ($\partial\beta/\partial E$) is larger than the value predicted by eq 17, by roughly the same multiplicative factor.[32] [It is important to emphasize that the deviation from the Marcus prediction cannot be attributed to double-layer effects, since the Frumkin correction for neutral reactants causes both β and $\partial\beta/\partial E$ to move in the same direction.[33,34]] Indeed, we will show that the deviation of the heterogeneous rate data from the Marcus prediction has the same functional dependence on ΔG, as has commonly been observed in a variety of homogeneous systems.

Table IV. Intrinsic Barriers Calculated from the Rehm-Weller Relationship Using the Transfer Coefficient (Eq 19) or the Curvature (Eq 20)

alkylmetal	$\Delta G^{\ddagger}$ (kcal mol^{-1})	β	$\partial\beta/\partial\Delta G$ (kcal^{-1} mol)	$\Delta G_0^{\ddagger}$ (kcal mol^{-1}) eq 19	eq 20	$\Delta\tilde{G}_0^{\ddagger}$[a] (kcal mol^{-1})
Et_4Sn	8.00	0.34	0.032	11	8	9
(*sec*-Bu)$_4$Sn	8.47	0.29	0.032	13	8	10
(*i*-Bu)$_4$Sn	7.97	0.30	0.032	12	8	10

[a] Geometric mean of the values in columns 5 and 6.

Table V. Intrinsic Barriers Calculated from the Modified Marcus Equation

alkylmetal	$\Delta G^{\ddagger}$ (kcal mol^{-1})	β	$(\partial\beta/\partial\Delta G)$ (kcal^{-1} mol)	$\Delta G_0^{\ddagger}$[a] (kcal mol^{-1}
Et_4Sn	8.00	0.34	0.032	10
(*sec*-Bu)$_4$Sn	8.47	0.29	0.032	12
(*i*-Bu)$_4$Sn	7.97	0.30	0.032	11

[a] Calculated from eq 22.

B. $\Delta G_0^{\ddagger}$ from the Rehm–Weller Formulation. We now evaluate the capability of the empirical relationship proposed by Rehm and Weller in eq 18,[37] to reproduce the activation free energy over

$$\Delta G^{\ddagger} = \frac{\Delta G}{2} + \left[\left(\frac{\Delta G}{2}\right)^2 + (\Delta G_0^{\ddagger})^2\right]^{1/2} \qquad (18)$$

a wide potential range, in which eq 13 fails. Although eq 18 was originally proposed for homogeneous rate processes, we apply it to the heterogeneous electrode process by proceeding in a manner analogous to that used for eq 13. Thus it is again possible to obtain two independent measures of $\Delta G_0^{\ddagger}$ from the magnitude and the slope of β. Equation 19 which is analogous to eq 16, yields $\Delta G_0^{\ddagger}$

$$\Delta G_0^{\ddagger} = \Delta G^{\ddagger}\left(\left|\frac{2\beta - 1}{\beta}\right|\right)[(4\beta - 2)^{-2} - \tfrac{1}{4}]^{1/2} \qquad (19)$$

on the basis of the magnitude of β. In the second procedure, $\Delta G_0^{\ddagger}$ depends inversely on the slope $\partial\beta/\partial E$ according to eq 20, which

$$\Delta G_0^{\ddagger} = \left[\left|\frac{(4\beta - 2)^3}{16} + \beta - \frac{1}{2}\right|\right][(4\beta - 2)^{-2} - \tfrac{1}{4}]^{1/2}\,(\partial\beta/\partial\Delta G)^{-1} \qquad (20)$$

is analogous to eq 17. [The derivation of these equations is given in the Experimental Section.] The results of the computations presented in Table IV (columns 5 and 6) show considerable improvement in the coincidence of $\Delta G_0^{\ddagger}$ evaluated from β and $\partial\beta/\partial E$. It should be noted that the geometric mean in column 7 is again quite akin to $\Delta G_0^{\ddagger}$ obtained from the homogeneous iron(III) data. Although the Rehm–Weller formulation is closer to the correct functional relationship beteen $\Delta G^{\ddagger}$ and $\Delta G_0^{\ddagger}$, as an empirical equation it does not lend any additional insight as to the causes of the failure of eq 13 over an extended potential range.[38] However, we can draw one conclusion important to this study; viz., the causes which necessitated Rehm and Weller to propose their eq 18 to fit the homogeneous electron-transfer data are common to the heterogeneous electrode process, certainly as it applies to organometals.

(31) See the Experimental Section for the derivation of this equation.
(32) (a) Note that an arithmetic average would indicate an additive factor. (b) The intrinsic barriers for electron transfer $\Delta G_0^{\ddagger}$ obtained from the homogeneous and heterogeneous rate data will differ by the reorganization energy for the iron(III) oxidant. However, the latter is quite small (especially in comparison with the magnitude of $\Delta G_0^{\ddagger}$ of 10 kcal mol^{-1}), based on the reported self-exchange rate of 3×10^8 M^{-1} s^{-1} for (bipy)$_3$Fe^{3+} in ref 47.
(33) Mohilner, D. M. *J. Phys. Chem.* **1969**, *73*, 2653. See also ref 26.
(34) (a) Indeed the same quantitative tendency has been noted previously. Thus, Saveant has recently reported that the observed β was smaller and $\partial\beta/\partial E$ larger than those predicted by the quadratic Marcus relationship, despite extensive corrections for the double layer effect.[26] (b) It has also been suggested that values of $\partial\beta/\partial E$ larger than the Marcus prediction for electrochemical systems may be due to surface effects.[35] However, similar problems are extant in the literature for homogeneous electron-transfer processes.[36]
(35) Angell, D. H.; Dickinson, T. *J. Electroanal. Chem.* **1972**, *35*, 55. Samec, Z.; Weber, J. *Ibid.* **1977**, *77*, 163.
(36) Scandola, F.; Balzani, V. *J. Am. Chem. Soc.* **1979**, *101*, 6140.
(37) Rehm, D.; Weller, A. *Ber. Bunsenges. Phys. Chem.* **1969**, *73*, 834.
(38) Since a second empirical relationship, originally proposed by Marcus, R. A. [*J. Phys. Chem.* **1968** *72*, 891], for atom-transfer processes and later modified for electron transfer reactions,[36] is seen to afford with organometals results which are intermediate between the Marcus and the Rehm–Weller equations, it will not be discussed further. See also: Agmon, N.; Levine, R. D. *Chem. Phys. Lett.* **1977**, *52*, 197.

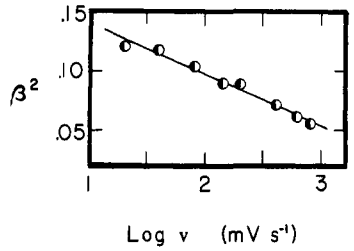

Figure 10. Verification of eq 23, showing the functional relationship of the transfer coefficient (β^2) and the CV sweep rate (log v) for n-Bu_4Sn,[41] in acetonitrile containing 0.1 M TEAP at 25 °C.

C. $\Delta G_0^{\ddagger}$ from the Modified Marcus Equation. Owing to its theoretical significance, it would be advantageous to find a mathematical form of the Marcus eq 13 which would tend to minimize the error in its use to evaluate $\Delta G_0^{\ddagger}$. Since the result in Table III indicates that the errors in β and $\partial\beta/\partial\Delta G$ are coupled by the same multiplicative factor, a mathematical formulation of eq 13 in which these parameters appear only as a ratio will reduce the problems inherent to systems far removed from the equilibrium potential. This is most conveniently done by obtaining the free-energy change as a function of the first and second derivatives of eq 13, e.g.,[31]

$$\Delta G = (\beta - \tfrac{1}{2})/(\partial\beta/\partial\Delta G) \qquad (21)$$

Substitution of eq 21 into the Marcus eq 13, followed by rearrangement, yields:

$$\Delta G_0^{\ddagger} = \Delta G^{\ddagger} - \frac{1}{2}\frac{(\beta - \tfrac{1}{2})}{(\partial\beta/\partial\Delta G)} - \frac{1}{16\Delta G_0^{\ddagger}}\frac{(\beta - \tfrac{1}{2})^2}{(\partial\beta/\partial\Delta G)^2} \qquad (22)$$

[See the Experimental Section for the mathematical manipulation of the Marcus eq 13 into eq 22.] Values of $\Delta G_0^{\ddagger}$ calculated from eq 22 are presented in Table V, column 5. Indeed the values of $\Delta G_0^{\ddagger}$ obtained in this manner are strikingly close to those obtained from the homogeneous chemical rate data.

IV. Nature of the Transfer Coefficient. Figure 9 underscores the essential concordance of α and β. Since the slope of the plot $\partial\beta/\partial\Delta G = \partial\alpha/\partial\Delta G = (8\Delta G_0^{\ddagger})^{-1}$ according to eq 17, the parameters α and β must be characteristic of the structural identity of the particular organometal. In order to establish this relationship, we equate the activation free energy determined from the CV experiment with that predicted by the Marcus theory by combining eq 2, 14, and 16 to yield:[39]

$$\beta^2 = \frac{RT}{4\Delta G_0^{\ddagger}} \ln\left[2.18\left(\frac{D\beta nFv}{RT}\right)^{1/2}/Z\right] \qquad (23)$$

An experimental verification of eq 23 derives from the linear dependence of the transfer coefficient (β^2) on the CV sweep rate (log v) for a given organometal, as shown in Figure 10 for n-Bu_4Sn.

For a series of organometals, eq 23 also indicates that an inverse relationship exists between the intrinsic barrier $\Delta G_0^{\ddagger}$ and the transfer coefficient (β^2) when they are evaluated at a constant CV sweep rate.[40] [Note: According to eq 2, the CV measurements made at a constant sweep rate correspond to constant rates of electron transfer, i.e., constant, $\Delta G^{\ddagger}$. Thus the inverse relationship between β^2 and $\Delta G_0^{\ddagger}$ is also apparent from eq 16.] Indeed, this remarkable and useful prediction is borne out by the constancy of $\beta^2\Delta G_0^{\ddagger}$, as listed in the last column of Table VI.

Table VI. Effect of the Organometal Structure on the Transfer Coefficient and the Intrinsic Barrier[a]

alkylmetal	$\Delta G^{\ddagger}$ [b] (kcal mol^{-1})	β[c]	$\Delta G_0^{\ddagger}$ [d] (kcal mol^{-1})	$\beta^2\Delta G_0^{\ddagger}$ (kcal mol^{-1})
$Me_2Co(DpnH)$	7.46	0.73	2.1[e]	1.1
$(sec\text{-}Bu)_4Sn$	7.65	0.31	10.0	1.0
Et_4Pb	7.68	0.28	10.0	0.8
$Me_2Pt(PMe_2Ph)_2$	7.69	0.27	13.0	0.9
EtHgMe	7.70	0.20	22.0	0.9

[a] Measured with a stationary platinum microelectrode at 100 mV s^{-1} in acetonitrile containing TEAP as supporting electrolyte at 25 °C. [b] Calculated according to eq 2 and 14. [c] Calculated from the width of the wave according to eq 5. [d] Calculated as the geometric mean of the results from eq 16 and 17. [e] See footnote 42b.

It is interesting to note that the intrinsic barrier for the octahedral dimethylcobalt(III) macrocycle is significantly less than those for either the tetrahedral tetraalkyltin and lead compounds or the square-planar dimethylplatinum(II) complex. Furthermore the linear methylethylmercury has the largest value of $\Delta G_0^{\ddagger}$. The apparent inverse relationship of the intrinsic barrier with the coordiantion number and steric accessibility of the organometal suggests that solvation changes make important contributions to $\Delta G_0^{\ddagger}$.[42] However, a further elaboration on such structural effects awaits the examination of a wider variety of organometallic complexes and a more thorough study of solvents.

Summary and Conclusions

The homogeneous and the heterogeneous rates of electron transfer are measured under standard reaction conditions for four structurally diverse classes of organometallic complexes, I–IV. The second-order rate constants k_h for the *homogeneous* oxidation of homologous organometals can be extended up to the stopped-flow limit of 10^6 M^{-1} s^{-1}, using a series of phenanthroline iron(III) oxidants with standard reduction potentials ranging from 0.9 to 1.2 V. The *heterogeneous* rate constants k_e for electron transfer from the same organometals to a platinum electrode cannot be reliably measured below about 1.5 V, owing to the experimental limitations of measuring small CV currents.

The connection between the homogeneous and the heterogeneous rate processes is shown by the correlation in Figure 9 of the chemical Brønsted coefficient α and the electrochemical transfer coefficient β. However, the direct comparison of the homogeneous and heterogeneous activation barriers requires that the gap in the potentials be spanned since $\Delta G_h^{\ddagger}$ and $\Delta G_e^{\ddagger}$ must be simultaneously evaluated at the same thermodynamic driving force, i.e., potential. The free-energy relationship required to span this gap may be considered in the general form as:

$$\Delta G^{\ddagger}(E) = \Delta G^{\ddagger}(E_p) + \beta nF(E_p - E) + A_2(E_p - E)^2 + \ldots \qquad (24)$$

in which the activation free energy $\Delta G^{\ddagger}(E)$ evaluated at the standard potential of the iron(III) oxidant can be represented in terms of the activation free energy $\Delta G^{\ddagger}(E_p)$ at the experimentally determined CV peak potential together with a polynomial expansion in terms of the potential gap $(E_p - E)$. Accordingly in

(39) For clarity, it was assumed that $\partial w^p/\partial E \sim 0$ in the derivation of eq 23. See footnote 25b.

(40) An alternative view of this interrelationship among $\Delta G_0^{\ddagger}$, β, and v is elaborated in the Experimental Section.

(41) (a) In Figure 10, the term $1/2 \ln \beta$ on the right side of eq 23 may be considered as a simple constant in comparison to β^2 on the left side. (b) The predicted value of $4\beta^2\Delta G_0^{\ddagger}$ is 7.7 kcal mol^{-1} for $\Delta G^{\ddagger}$ from eq 16, which differs from the measured average value of 3.7 kcal mol^{-1}. However, if the Rehm–Weller relationship is employed, the corresponding value of $\Delta G^{\ddagger}$ is given by: $\Delta G_0^{\ddagger}(|\beta/(1-2\beta)|)[(4\beta-2)^{-2} - {}^1/_4]^{-1/2}$, which is in reasonable agreement with the measured average value of 7 kcal mol^{-1}.

(42) (a) The trend of $\Delta G_0^{\ddagger}$ in Table VI may be approximated by an outer-sphere energy term, if $\Delta G_{outer}^{\ddagger} = \Delta G_d^{\ddagger} + \Delta G_{coord}^{\ddagger}$. For example, $\Delta G_d^{\ddagger}$ evaluated on the basis of a dielectric continuum model is 2.2 kcal mol^{-1} for the dimethylcobalt(III) macrocycle.[21] For the solvation term $\Delta G_{coord}^{\ddagger}$, compare the solvent model of Drago.[44] Since the trend in $\Delta G_0^{\ddagger}$ exhibits no clear correlation with the mean bond energy of the alkylmetal bond,[43] it is unlikely to arise from differences in inner-sphere reorganization energies. (b) We wish to point out that the value of $\Delta G_0^{\ddagger}$ of 2.1 kcal mol^{-1} in Table VI is actually a lower limit. Thus we have recently shown that when the effect of reversibility is taken into account, the value of $\Delta G_0^{\ddagger}$ for the rate-limiting electron transfer is 6.3 kcal mol^{-1}. The validity of the arguments presented herein is essentially unaffected by electron transfer reversibility, which will be published separately at a later time.

(43) Kochi, J. K. "Organometallic Mechanisms and Catalysis"; Academic Press: New York, 1978, Chapter 11.

(44) Nozari, M. S.; Drago, R. S. *J. Am. Chem. Soc.* **1972**, *94*, 6877.

eq 24, when the second-order coefficient A_2 is zero, the free-energy relationship reduces to the linear function expressed in eq 3. Indeed, the use of such a linear free-energy relationship to span the potential gap allows a comparison of the homogeneous and heterogeneous rate processes to be made.[3] More importantly, when the free-energy relationship is expressed by the Marcus eq 13, the second-order coefficient A_2 is $(nF)^2/16\Delta G_0^{\ddagger}$, and then there is a direct one-to-one correspondence of the homogeneous and the heterogeneous rate processes, as shown in Figure 7. Marcus theory thus provides a quantitative means of relating the activation barriers for homogeneous and heterogeneous processes, when both proceed by outer-sphere mechanisms.

Since the potential gap $(E_p - E)$ in eq 24 is an important factor in allowing the homogeneous and heterogeneous rate processes to be compared, we might ask how its magnitude affects the first- and second-order contributions to the activation free energy. The largest gap occurs with the most resistant alkylmetal Et_4Si ($E_p - E$ = 1.58 V), in which the first-order term is 11 kcal mol^{-1} in contrast to the second-order term of only 3 kcal mol^{-1}. Thus even a relatively large error in the Marcus estimate for the second-order term in eq 24 will produce only a relatively small error in $\Delta G^{\ddagger}$. On the other hand, the converse situation is encountered when the Marcus formulation is used to evaluate the intrinsic barrier $\Delta G_0^{\ddagger}$ from the first- and second-order terms with eq 16 and 17, respectively.[45] Although $\Delta G_0^{\ddagger}$ for systems with small displacements from the equilibrium potential are well provided, those farther removed are better accommodated by the Rehm–Weller formulation. Analysis of the discrepancy suggests that the Marcus eq 13 predicts first derivatives (β) which are slightly too large and second derivatives ($\partial\beta/\Delta G$) which are too small. Thus the modified Marcus eq 22 presented in terms of the ratio of β and $\partial\beta/\partial\Delta G$ provides a particularly useful description of systems further removed from the equilibrium potential.

Experimental Section

Materials. The preparations of the organometallic complexes used in this study were described previously.[4,5] Reagent grade acetonitrile (Fisher Chemical Co.) was further purified by refluxing it over calcium hydride, then treated with potassium permanganate and redistilled from P_2O_5 through a 19-plate bubble cap Oldershaw column. Tetraethylammonium perchlorate (TEAP) was obtained from G. F. Smith Chemical Co. and dried in vacuo at 60 °C.

Electrochemical Measurements. The potentiostat and the electrochemical cell for cyclic voltammetry have been described previously.[3,46] For the convolutive potential sweep voltammetry, the current–time data were collected in digital form by sampling the current every 50 ms, which gave 150–200 data points for each scan. The convolution integral in eq 25, was evaluated by conversion to the finite summation in eq 26, where

$$\Psi(t) = \pi^{-1/2} \int_0^t i(\eta)(t - \eta)^{-1/2}\, d\eta \tag{25}$$

$$\Psi(t) = (\theta/\pi)^{1/2} \sum_{n=0}^{m} a_{n+1}\, i_{m-n} \tag{26}$$

θ is the time interval between the data points, m is the number of subintervals within the time period t defined according to $m = t/\theta$. The current i_{m-n} is evaluted at the time $\theta(m - n)$, and the coefficients a_n are obtained according to the relationship

$$a_n = (4n\sqrt{n} + (8 - 8n)\sqrt{n-1} + (4n - 8)\sqrt{n-2})/3 \tag{27}$$

which only applies for $n > 1$ (note: $a_1 = 4/3$). Integration with the coefficients defined by eq 27 is exact if the current can be considered to be a linear function of the time within the subintervals of length θ. This will always be true for a sufficiently short time interval. In practice, the values obtained from eq 27 were found to be rather insensitive to the coarseness of the time grid θ, provided the wave was divided into at least 20 intervals. The resultant convolution integral – time data was converted into the corresponding convolution integral – potential set by noting that $E = E_i + vt$, where E_i and v are the initial potential and the sweep rate, respectively. Finally, the area of the electrode was determined from the limiting value Ψ_L of the convolution integral in which case eq 6 (see Results) reduces to:

$$k_e(E) = D^{1/2} i(E)/(\Psi_L - \Psi_E) \tag{28}$$

as discussed by Imbeaux and Saveant.[14] The Fortran program for evaluating eq 26–28 was tested with the theoretical current–potential data tabulated by Nicholson and Shain[9] for a totally irreversible CV wave, and it is available upon request.

Derivation of Special Relationships from the Quadratic Marcus Equation. a. Derivation of Eq 16. The first derivative of the Marcus eq 13 with respect to the free-energy change ΔG yields the transfer coefficient

$$\beta = \tfrac{1}{2} + (\Delta G + w^p)/8\Delta G_0^{\ddagger} \tag{29}$$

which may be rearranged to:

$$2\beta - 1 = (\Delta G + w^p)/4\Delta G_0^{\ddagger} \tag{30}$$

Equation 30 upon substitution into eq 13 yields:

$$\Delta G^{\ddagger} = 4\beta^2 \Delta G_0^{\ddagger} \tag{16}$$

In this and all subsequent calculations, the work terms will be assumed to be independent of the free-energy change.[25,30] For the neutral molecules treated here, the work term of the reactant was assumed to be negligible.

b. Derivation of Eq 17. The derivative of eq 29 with respect to the free-energy change yields eq 17 directly.

c. Derivation of Eq 22. The combination of eq 30 and eq 17 yields the expression:

$$\Delta G + w^p = (\beta - \tfrac{1}{2})/(\partial\beta/\partial\Delta G) \tag{21}$$

relating the free energy change to the transfer coefficient and the potential dependence of β. Substitution of eq 21 into eq 13 produces the result in eq 22.

Derivation of the Special Relationships from the Rehm–Weller Equation. a. Derivation of Eq 19. The first derivative of the Rehm–Weller eq 18, with respect to ΔG, yields the transfer coefficient,

$$\beta = \frac{1}{2} + \frac{\Delta G}{4}\left[\left(\frac{\Delta G}{2}\right)^2 + (\Delta G_0^{\ddagger})^2\right]^{-1/2} \tag{31}$$

which can be rearranged to:

$$\Delta G/(4\beta - 2) = [(\Delta G/2)^2 + (\Delta G_0^{\ddagger})^2]^{1/2} \tag{32}$$

Substitution of eq 32 into the Rehm–Weller eq 18, followed by rearrangement, gives the expression for the free-energy change as:

$$\Delta G = [(2\beta - 1)/\beta]\Delta G^{\ddagger} \tag{33}$$

The intrinsic barrier according to eq 19 is then obtained from the solution of eq 33 and 32.

b. Derivation of Eq 20. The derivative of eq 31 with respect to the free-energy change is:

$$\partial\beta/\partial\Delta G = -\tfrac{1}{16}[(\Delta G/2)^2 + (\Delta G_0^{\ddagger})^2]^{-3/2}\Delta G^2 + \tfrac{1}{4}[(\Delta G/2)^2 + (\Delta G_0^{\ddagger})^2]^{-1/2} \tag{34}$$

The terms in the brackets are eliminated by the use of eq 32 to give:

$$\partial\beta/\partial\Delta G = [-\tfrac{1}{16}(4\beta - 2)^3 + \tfrac{1}{4}(4\beta - 2)]/\Delta G \tag{35}$$

The expression for the free-energy change ΔG is obtained from eq 32 as:

$$\Delta G_0^{\ddagger} = (|\Delta G|)[(4\beta - 2)^{-2} - \tfrac{1}{4}]^{1/2} \tag{36}$$

Substitution of eq 36 into eq 35 yields the final result in eq 20.

Linear Correlation of the Homogeneous and Heterogeneous Rate Constants for Electron Transfer from the Marcus Equation. For the homogeneous oxidation of an organometal (species 1) by a chemical oxidant (species 2), the expansion of the Marcus eq 13 yields:

$$\Delta G_h^{\ddagger} = \frac{1}{2} w_h^p + \Delta G_{0h}^{\ddagger} + \frac{\Delta G}{2} + \frac{[\Delta G + w_h^p]^2}{16\Delta G_{0h}^{\ddagger}} \tag{37}$$

where $\Delta G = (\Delta G_1 - \Delta G_2)$ represents the difference in the free-energy changes for the organometal and oxidant. The corresponding activation free energy for the heterogeneous oxidation of the organometal is:

$$\Delta G_e^{\ddagger} = \frac{1}{2} w_e^p + \Delta G_{01}^{\ddagger} - \frac{nF}{2}(E - E_1^0) + \frac{[-nF(E - E_1^0) + w_e^p]^2}{16\Delta G_{01}^{\ddagger}} \tag{38}$$

The combination of eq 37 and 38 when they are evaluated at the standard reduction potential of species 2 (i.e., at $E = E_2^0$) yields:

(45) When the second-order term is small, errors in the curvature are magnified in the evaluation of $\Delta G_0^{\ddagger}$. The same is true of the linear term.

(46) Van Duyne, R. P.; Reilley, C. N. *Anal. Chem.* **1972**, *44*, 142.

$$\Delta G_e^{\ddagger}(E_2^0) = \Delta G_h^{\ddagger} - \Delta G_{02}^{\ddagger} + \Delta_{cur} + \Delta_{work} + \Delta_{reorg} \quad (39)$$

where the last three designations represent the correction terms.

For an outer-sphere electron transfer, eq 39 predicts that a plot of the homogeneous activaton free energy against the heterogeneous activation free energy evaluated at the standard potential of the oxidant would be linear with a slope of unity, provided the three correction terms are independent of the free-energy change. While this proviso is likely to be a good approximation for Δ_{work} and Δ_{reorg}, the value of Δ_{cur} as given by:

$$\Delta_{cur} = \frac{[\Delta G + w_e^P]^2}{16\Delta G_{01}^{\ddagger}} - \frac{[\Delta G + w_h^P]^2}{16\Delta G_{0h}^{\ddagger}} \quad (40)$$

depends on the square of the free-energy change. Equation 40 may be approximated by eq 41 when the intrinsic barrier for the oxidant is much

$$\Delta_{cur} \simeq \Delta G_{02}^{\ddagger}(16\Delta G_h^{\ddagger}\Delta G_{01}^{\ddagger})^{-1}[\Delta G + w_h^P]^2 \quad (41)$$

smaller than that of the organometal. Indeed this approximation is valid for the system examined here. Thus an upper limit of 2 kcal mol^{-1} can be placed on $\Delta G_{02}^{\ddagger}$ from the reported self-exchange rate of 3×10^8 M^{-1} s^{-1} for tris(bipyridine)iron(III).[47] This value compares with $\Delta G_{01}^{\ddagger}$ of 10 kcal mol^{-1}, determined previously.[6] Using these values of $\Delta G_{02}^{\ddagger}$ and $\Delta G_{0h}^{\ddagger} = \Delta G_{01}^{\ddagger}$, the upper limits for Δ_{cur} are calculated to be typically 0.4, 0.3, and 0.2 kcal mol^{-1} for Et_4Si at E = 0.98, 1.08, and 1.18 V vs. SCE and 0.4, 0.2, and 0.1 kcal mol^{-1} for Et_4Sn at E = 0.98, 1.08, and 1.18 V. Thus the comparison with the homogeneous activation free energies shows that the contribution from Δ_{cur} is minor, and the uncertainty in $\Delta G_{02}^{\ddagger}$ is of small consequence.

The correction terms Δ_{work} and Δ_{reorg} which are evaluated from the Marcus eq 13 as $(w_e^P - w_h^P)/2$ and $(\Delta G_{01}^{\ddagger} + \Delta G_{02}^{\ddagger} - \Delta G_{0h}^{\ddagger})$, respectively, contribute to the intercept in Figure 7. The work term correction, Δ_{work}, may be estimated on the basis of existing theoretical models. Thus the homogeneous work term w_h^P is evaluated as $\sim$2 kcal mol^{-1} from the Sutin–Brown treatment,[48] taking the dielectric constant as 37.5 and an arbitrary ion-pair separation of 11 Å. The heterogeneous work term w_e^P is estimated to be 6 kcal mol^{-1}, based on the assumption that the double layer potential of platinum is the same as that of mercury[49] and symmetric about zero. Since one-half of the difference accounts for almost all of the intercept (2.6 kcal mol^{-1}) in Figure 7, the contribution for Δ_{reorg} appears to be small.[50]

Effect of the Intrinsic Barrier on the Transfer Coefficient and the CV Peak Potential. The transfer coefficient, the CV sweep rate, and the intrinsic barrier are the three parameters in eq 23 which relate the heterogeneous rate constants for electron transfer determined by the CV method with the Marcus theory. In order to understand their interrelationship, it is important to emphasize that the rate of electron transfer at the CV peak potential E_p is fixed by the sweep rate according to eq 2. Thus for a typical sweep rate of 100 mV s^{-1}, the CV peak potential will occur at the point where k_e = 0.010 cm s^{-1}, by taking β = 0.5 and $D = 1 \times 10^{-5}$ cm^2 s^{-1}. This value of k_e corresponds to $\Delta G_e^{\ddagger}$ of 7.7 kcal mol^{-1}. Therefore at 100 mV s^{-1}, the CV peak potential will occur at the standard reduction potential E^0 only if the intrinsic barrier equals 7.7 kcal mol^{-1}. In other words, at this standard reduction potential, the free-energy change ΔG is zero, and it follows that $\Delta G^{\ddagger} = \Delta G_0^{\ddagger}$ according to the Marcus eq 13.

For smaller barriers, ΔG must then be larger (since $\Delta G^{\ddagger} = \Delta G_0^{\ddagger} + \Delta G/2$)[51] and E_p will occur prior to E^0 (i.e., at more negative potentials in an oxidation). In this endergonic region of the free-energy curve, the Marcus quadratic relationship predicts transfer coefficients greater than 0.5 from the relationship $\beta = \partial\Delta G^{\ddagger}/\partial\Delta G = {}^1/_2 + \Delta G/(8\Delta G_0^{\ddagger})$, as indeed shown by $Me_2Co(DpnH)$ in Table VI. By a similar line of reasoning, for intrinsic barriers greater than 7.7 kcal mol^{-1}, the CV wave will occur in the exergonic region and exhibit transfer coefficients less than 0.5, as indded shown by *sec*-Bu_4Sn and Et_4Pb in Table VI.

Acknowledgment. We wish to thank the National Science Foundation for financial support of this research.

Supplementary Material Available: Tables I-S to IV-S listing homogeneous rate constants and activation free energies as well as calculated heterogeneous activation free energies for the oxidation of organometals (4 pages). Ordering information is given on any current masthead page.

(47) (a) Pladziewicz, J. R.; Espenson, J. H. *J. Am. Chem. Soc.* **1973**, *95*, 56. (b) Assuming the work term is zero.

(48) Brown, G. M.; Sutin, N. *J. Am. Chem. Soc.* **1979**, *101*, 883. [Refer to eq 24 in this paper.]

(49) (a) See footnotes 25 and 26. (b) For the effects of the double layer, see: Delahay, P. in ref 30, pp 42 and 197; Mareček, V.; Samec, Z.; Weber, J. *J. Electroanal. Chem.* **1978**, *94*, 169.

(50) (a) The small residual discrepancy of $\sim$1 kcal mol^{-1} in the intercept may be readily included in Δ_{reorg}, using eq 20 and 21 cited by Weaver in ref 2d and from Marcus.[21] The ambiguity in the separation parameter to be used introduces errors far in excess of this discrepancy. (b) Errors in the evaluation[22] of the frequency factors Z_e and Z_h also no doubt contribute to the intercept.

(51) For clarity of emphasis, the linear relationship is employed here.